Earthquakes and Structures, *Vol. 8, No. 5 (2015) 957-976*
DOI: http://dx.doi.org/10.12989/eas.2015.8.5.957

Correlation of elastic input energy equivalent velocity spectral values

Yin Cheng, Andrea Lucchini and Fabrizio Mollaioli*

Department of Structural and Geotechnical Engineering, Sapienza University of Rome, Via Gramsci 53, Rome, Italy

(Received February 27, 2014, Revised May 19, 2014, Accepted August 13, 2014)

Abstract. Recently, two energy-based response parameters, i.e., the absolute and the relative elastic input energy equivalent velocity, have been receiving a lot of research attention. Several studies, in fact, have demonstrated the potential of these intensity measures in the prediction of the seismic structural response. Although some ground motion prediction equations have been developed for these parameters, they only provide marginal distributions without information about the joint occurrence of the spectral values at different periods. In order to build new prediction models for the two equivalent velocities, a large set of ground motion records is used to calculate the correlation coefficients between the response spectral values corresponding to different periods and components of the ground motion. Then, functional forms adopted in models from the literature are calibrated to fit the obtained data. A new functional form is proposed to improve the predictions of the considered models from the literature. The components of the ground motion considered in this study are the two horizontal ones only. Potential uses of the proposed equations in addition to the prediction of the correlation coefficients of the equivalent velocity spectral values are shown, such as the prediction of derived intensity measures and the development of conditional mean spectra.

Keywords: correlation coefficient; input energy equivalent velocity spectra; conditional mean spectrum

1. Introduction

Since the study of Housner (1956) on seismic energy in structures was published, many efforts have been spent for defining and applying energy-based approaches in procedures for seismic design and seismic assessment of structures (e.g., Akiyama 1985, Krawinkler 1987, McCabe and Hall 1989, Fajfar and Vidic 1994, Chou and Uang 2000, Chou and Uang 2003). A variety of energy parameters has been studied. Among others, Uang and Bertero (1990) investigated two types of input energy demand parameters as measures of the earthquake intensity and potential predictors of seismic demand: the absolute and the relative input energy. Input energy demands have been shown to be good parameters for designing earthquake-resistant structures, especially for those cases in which duration-related cumulative damage below the maximum response (i.e., cyclic damage) is significant. These energy-based parameters, in fact, are related to the cycles of response of the system (e.g., see Fajfar and Fischinger 1990, Decanini and Mollaioli 1998,

*Corresponding author, Professor, Ph.D., E-mail: fabrizio.mollaioli@uniroma1.it

http://www.techno-press.org/journals/eas&subpage=7 ISSN: 2092-7614 (Print), 2092-7622 (Online)

Manfredi 2001), as opposed to parameters, such as the pseudo-acceleration, related to the peak value of the seismic demand. Therefore these energy-based parameters implicitly capture the effect of ground motion duration, which is not accounted for by the conventional spectral parameters. The good prediction capability of the energy parameters in general, is mainly due to the fact that their values do not only depend on the amplitude, frequency content, and duration of the ground motion, but also on the dynamic properties of the structure.

Several types of elastic and inelastic energy-based spectra have been developed and applied for the evaluation of the seismic performance of structures (Decanini and Mollaioli 2001, Chai and Fajfar 2000, Benavent-Climent *et al*. 2010, López-Almansa *et al*. 2013). Among these proposals, inelastic input energy spectra have been shown to be very efficient tools for the evaluation of the seismic demand of multi-degree-of-freedom structures experiencing damage. Numerous studies (e.g., Bertero and Uang 1992, Teran-Gilmore 1996) highlighted the influence of ductility on inelastic input energy spectra, i.e., the differences between inelastic and elastic input energy spectra, in relation with the considered period of vibration, the ground motion properties, and the soil conditions. In particular, it was found that the influence is reduced in the short periods region, while is more significant at periods corresponding to the maximum input energy values (Mollaioli *et al*. 2011). Despite these differences, however, also the elastic input energy has been found to be well correlated to the seismic demand. This was observed, for example, in the investigations of Mollaioli *et al*. (2011) on the prediction of displacement-related demand parameters (e.g., the maximum inter-story drift ratio) of multistory buildings.

Due to the above mentioned findings and to those of recent studies that proved the reduced predictive capabilities of commonly used intensity measures (IMs), such as, the pseudo-acceleration (*Sa*), the peak ground acceleration (*PGA*), and the peak ground velocity (*PGV*) (e.g., see the works of Yakut and Yilmaz 2008, Jayaram *et al*. 2010, Lucchini *et al*. 2011, Mollaioli *et al*. 2013), elastic input energy have received a renewed research attention in the performance-based earthquake engineering community. New alternative intensity measures derived from elastic input spectra have been proposed. Intensity measures obtained from spectral ordinates at different periods, consisting in vectors or combinations of spectral values, and from integration of the spectra over defined ranges of periods have been investigated (e.g., see the vector IMs studied in Luco *et al*. 2005, and the integral IMs considered in Mollaioli *et al*. 2013). By adopting this approach, higher modes contribution and elongation of the periods of vibration due to damage are explicitly accounted for, and consequently the prediction of the nonlinear response of MDOF structures can be improved.

In order to use these intensity measures derived from elastic input energy spectra in probabilistic seismic hazard and risk analyses, attenuation relationships and equations for the prediction of the correlation of spectral values are needed. In the literature, the absolute and relative input energies are frequently replaced with their equivalent velocities V_{EIa} and V_{EIr}. For these intensity measures several ground motion prediction equations (GMPE) can be found (i.e., see Chapman 1999, Gong and Xie 2005, Danciu and Tselentis 2007, Cheng *et al*. 2014).These GMPEs only consider the marginal distribution of individual spectral values without giving any information about the joint distribution of the spectral values at different periods. The correlation between the spectral values of other IMs, such as *Sa*, has been already investigated (e.g., see Baker and Cornell 2006b, Baker and Jayaram 2008, Abrahamson *et al*. 2003, Cimellaro 2013). However, works on the correlation of the V_{EIa} and V_{EIr} spectral values are still lacking.

The main purpose of this study is to propose models for the prediction of the correlation coefficients of the V_{EIa} and V_{EIr} spectral values. In order to pursue this objective, firstly, a dataset of correlation coefficients values will be derived from a database of ground motions records. Then, functional forms of equations adopted in the literature to predict other IMs will be calibrated to fit the V_{EIa} and V_{EIr} correlation coefficients data. Finally new predictive equations will be developed in order to improve the fitness between the observed data and the predicted values. For both V_{EIa} and V_{EIr}, the following correlations are investigated: the correlation between the two ordinates of the equivalent velocity spectrum of the single horizontal component of the ground motion; the correlation between the ordinates of the spectra of the two orthogonal horizontal components calculated at the same period value; the correlation between the ordinates of the spectra of the two orthogonal horizontal components calculated at two different periods. At the end of this study, some possible applications of the proposed equations will be shown. The prediction of V_{EI}-derived IMs using the proposed equations will be described. In addition, the use of such equations for the development of conditional mean spectra (see, e.g., Haselton *et al*. 2009) will be discussed.

2. Elastic input energy equivalent velocities

For a damped linear elastic single-degree-of-freedom (SDOF) system subjected to a ground motion, the dynamic equilibrium can be described with one of the two following equations

$$m\left(\ddot{x}_g + \ddot{x}\right) + c\dot{x} + kx = 0 \tag{1}$$

$$m\ddot{x} + c\dot{x} + kx = -m\ddot{x}_g \tag{2}$$

in which

$\ddot{x}_t = \ddot{x}_g + \ddot{x}$;

and where

x_g is the ground displacement;

x is the relative displacement with respect to the ground;

m is the mass of the oscillator;

c is viscous damping coefficient;

k is the stiffness of the oscillator.

By integrating Eqs. (1) and (2) with respect to x, the following energy balance equations can be easily derived (Uang and Bertero 1990)

$$E_{Ia}=E_{Ka}+E_{\xi}+E_S \tag{3}$$

$$E_{Ir}=E_{Kr}+E_{\xi}+E_S \tag{4}$$

in which

$E_{Ia} = \int m\ddot{x}_t dx_g$ is the absolute input energy;

$E_{Ir} = -\int m\ddot{x}_g dx$ is the relative input energy;

$E_{Ka} = \frac{1}{2} m\dot{x}_t^2$ is the absolute kinetic energy;

$E_{Kr} = \frac{1}{2} m\dot{x}^2$ is the relative kinetic energy;

$E_\xi = \int c\dot{x}dx$ is the damping energy;

$E_S = \frac{1}{2}kx^2$ is the elastic strain energy.

Eqs. (3) and (4) are usually called in the literature "absolute" and "relative" energy equation, respectively. The absolute input energy (E_{Ia}) can be explained as the work done by the total base shear force on the ground displacement, while the relative input energy (E_{Ir}) describes the work done by the static equivalent lateral force $\left(-m\ddot{x}_g\right)$ on the relative displacement of the SDOF with respect to the ground.

Analogously to what is done in Chou and Uang (2000) for the absorbed energy E_a, E_{Ia} and E_{Ir} can be converted into equivalent velocities as follows

$$V_{EIa} = \sqrt{2E_{Ia}/m} \tag{5}$$

$$V_{EIr} = \sqrt{2E_{Ir}/m} \tag{6}$$

with the absolute input energy equivalent velocity (V_{EIa}) and the relative input energy equivalent velocity (V_{EIr}) being independent on mass. In the following of the work, the values of the equivalent velocities used in the correlation analyses will be calculated using a damping ratio equal to 5%.

As shown in Fig. 1, the two equivalent velocities are very close in the intermediate periods range, and different at longer and shorter periods. In particular, V_{EIr} reduces significantly with the decrease of the period value, while V_{EIa} approaches to 0 at very long periods. These opposite trends can be easily explained with the two following considerations: for the limit case of a period value equal to 0, the relative displacement of the SDOF system (and therefore also E_{Ir}) tends to 0; on the contrary, for the limit case of an infinitely large period value, it is the total displacement (and therefore E_{Ia}) that tends to 0. The pseudo-velocity (*Spv*), which in the elastic case is equal to the equivalent velocity of the absorbed energy, is characterized by similar trends of that of V_{EIr} and

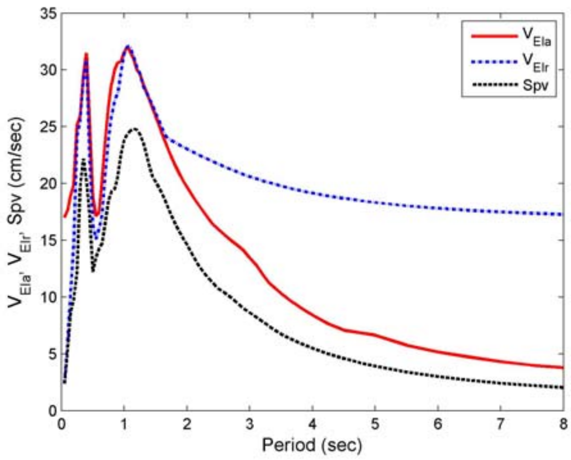

Fig. 1 Comparison between pseudo-velocity (*Spv*), absolute input energy equivalent velocity (V_{EIa}) and relative input energy equivalent velocity (V_{EIr}), calculated for Carroll College station record from Helena Montana earthquake on 31th Oct. 1935

V_{EIa} at short and long periods, respectively. Thus, V_{EIa} is asymptotic to *Spv* at long periods, while V_{EIr} is asymptotic to *Spv* at short periods.

3. Calculation of correlations

Given a dataset of ground motions, the input energy equivalent velocities of the two horizontal components of each record can be expressed in a logarithmic form as follows

$$\ln V_{EI\,x}(T) = f(M,R,T,\theta) + \sigma(T)\varepsilon_x(T) \tag{7}$$

$$\ln V_{EI\,y}(T) = f(M,R,T,\theta) + \sigma(T)\varepsilon_y(T) \tag{8}$$

where

V_{EI} represents the observed spectral value of V_{EIa} or V_{EIr} for the single considered record;

x and y denote the two orthogonal horizontal components of the record;

$f(M,R,T,\theta)$ is the predicted median of the logarithm of V_{EIa} or V_{EIr}, calculated at a specific period T using a selected GMPE, as a function of magnitude (M), source to site distance (R), and other parameters (θ);

σ is the standard deviation of the predicted V_{EIa} or V_{EIr}, which is provided by the GMPE;

ε measures (in terms of number of standard deviations σ) the difference between the observed value $\ln V_{EI}$ and the predicted median value $f(M,R,T,\theta)$. An ε value equal to 2, for example, denotes that the observed value corresponding to the considered record is two standard deviations larger than the median ground motion predicted based on the information on the causal earthquake event.

Eqs. (7) and (8) can be used to express ε in the following form

$$\varepsilon_x(T) = \frac{\ln V_{EI\,x}(T) - f(M,R,T,\theta)}{\sigma(T)} \tag{9}$$

$$\varepsilon_y(T) = \frac{\ln V_{EI\,y}(T) - f(M,R,T,\theta)}{\sigma(T)} \tag{10}$$

Based on the above equations, and on the fact that $f(M,R,T,\theta)$ and $\sigma(T)$ are defined as the median and standard deviation of $\ln V_{EI}(T)$, it derives that $\varepsilon_x(T)$ and $\varepsilon_y(T)$, which account for the randomness of the observed data, are characterized by a zero mean and a unit standard deviation. By looking at Eqs. (9) and (10), it can be noted that $\varepsilon(T)$ is linearly related to $\ln V_{EI}(T)$. Based on this observation, $\varepsilon(T)$ spectra can be calculated and used instead of those of $\ln V_{EI}(T)$ in order to appropriately evaluate the correlation of the equivalent velocities spectral values.

The correlation between the $\varepsilon(T)$ values at different periods can be estimated using the Pearson product-moment correlation coefficient

$$\rho_{\varepsilon(T_1),\varepsilon(T_2)} = \frac{\sum_{i=1}^{n}(\varepsilon_i(T_1) - \overline{\varepsilon(T_1)})(\varepsilon_i(T_2) - \overline{\varepsilon(T_2)})}{\sqrt{\sum_{i=1}^{n}(\varepsilon_i(T_1) - \overline{\varepsilon(T_1)})^2 \sum_{i=1}^{n}(\varepsilon_i(T_2) - \overline{\varepsilon(T_2)})^2}} \tag{11}$$

where

$\varepsilon_i(T_1)$ and $\varepsilon_i(T_2)$ is the ith observation of ε at T_1 and T_2, respectively;

n is the number of observations;
$\overline{\varepsilon(T_1)}$ and $\overline{\varepsilon(T_2)}$ are the sample means of all the n observations at T_1 and T_2, respectively.

Depending on the considered horizontal component of the ground motion and the selected period value, three different correlation coefficients can be evaluated: the correlation coefficient $\rho_{\varepsilon(T_1),\varepsilon(T_2)}$ between two ordinates of the $\varepsilon(T)$ spectrum of the single horizontal component of the ground motion; the correlation coefficient $\rho_{\varepsilon_x(T),\varepsilon_y(T)}$ between the ordinates of the spectra of the two orthogonal horizontal components calculated at the same period value; the correlation coefficient $\rho_{\varepsilon_x(T_1),\varepsilon_y(T_2)}$ between the ordinates of the spectra of the two orthogonal horizontal components calculated at two different periods.

The records used to empirically calculate the ρ values (which are then used to derive the proposed predictive equations) were collected from the NGA database. Only records with the following properties were selected: records with both the two horizontal components available; records characterized by a corner frequency value of the high-pass filter lower than 0.2 Hz and a low-pass filter corner frequency value higher than 18 Hz; records from earthquakes with magnitudes larger than 5, and closest distances lower than 200 km; records corresponding only to soil conditions type B, C and D (as classified according to NEHRP). Even though records from sites classified as type A and E are of interest (especially the latter, which can be characterized by energy demands several times larger than those corresponding to firm sites), they were excluded from the database because their number was not statistically sufficient for carrying out correlation analyses. Based on the previous criteria, 740 ground motions recorded from 40 earthquakes were identified. More detailed information about these records is given in Appendix (see Table B).

4. Empirical correlation coefficients and proposed predictive equations

Four GMPEs, namely, Chapman (1999), Gong and Xie (2005), Danciu and Tselentis (2007), Cheng *et al*. (2014) are used to calculate the correlation coefficients. Chapman (1999) used a set of records from 20 earthquakes in Western North America to develop the GMPE. A set of 266 records from 15 Californian earthquakes were considered in the study of Gong and Xie (2005). A dataset consisting of 335 records from 151 Greek earthquakes were used by Danciu and Tselentis (2007), while a dataset of 1550 records from 63 worldwide earthquakes (incuding many from Western North American) were considered in Cheng *et al*. (2014). Except for the case of Danciu and Tselentis (2007), the other GMPEs were developed on datasets of records that are consistent.

4.1 Correlation for the same component of spectral values at different periods

The empirical correlation coefficients $\rho_{\varepsilon(T_1),\varepsilon(T_2)}$ calculated for both V_{EIa} and V_{EIr} are shown in Figs. 2 and 4 and Figs. 3 and 5, respectively. In particular, Figs. 2-3 report the contour lines of the $\rho_{\varepsilon(T_1),\varepsilon(T_2)}$ surface as a function of T_1 and T_2, while in Figs. 4-5 the correlation coefficients are plotted as a function of T_1 for different period values of T_2.

By looking at the results obtained for V_{EIa}, it can be observed that the correlation coefficient is not significantly influenced by the choice of GMPE used to calculate it. The most evident difference is in the values obtained with Daciu and Tselentis (2007) compared to those obtained with the other GMPEs. The difference is probably due to the fact that in Danciu and Tselentis (2007) only records from Greece are used to derive the GMPE, while in the other studies the datasets of records are dominated by Califonian earthquakes. In addition, the GMPE of Danciu and

Tselentis (2007) was developed without explicitly taking into account the magnitude saturation phenomenon, as done on the contrary in the other studies, resulting in a different shape of the median input energy spectrum (see Cheng *et al.* 2014). As shown in Figs. 3 and 5, the same reduced influence on $\rho_{\varepsilon(T_1),\varepsilon(T_2)}$ of the used GMPE can be observed also for V_{EIr}. In this case only the results obtained with Gong and Xie (2005) and Cheng *et al*. (2014) are compared since in the other studies GMPEs for V_{EIr} were not developed. By comparing the plots of Figs. 2 and 3, and those of Figs. 4 and 5, it is interesting to note that, in general, the values of the correlation coefficient obtained for V_{EIa} are larger than those obtained for V_{EIr}. This trend may be in part explained by the fact that at very short periods the V_{EIr} value tends to zero independently on the considered ground motion, while that of V_{EIa} is sensitive to it. This property of V_{EIr}, has been previosuly shown in the spectra of Fig. 1, and discussed at the end of section 2. As a direct consequence, correlation between the values of the equivalent velocities at short periods and those at medium and long periods is lower for V_{EIr} than for V_{EIa}.

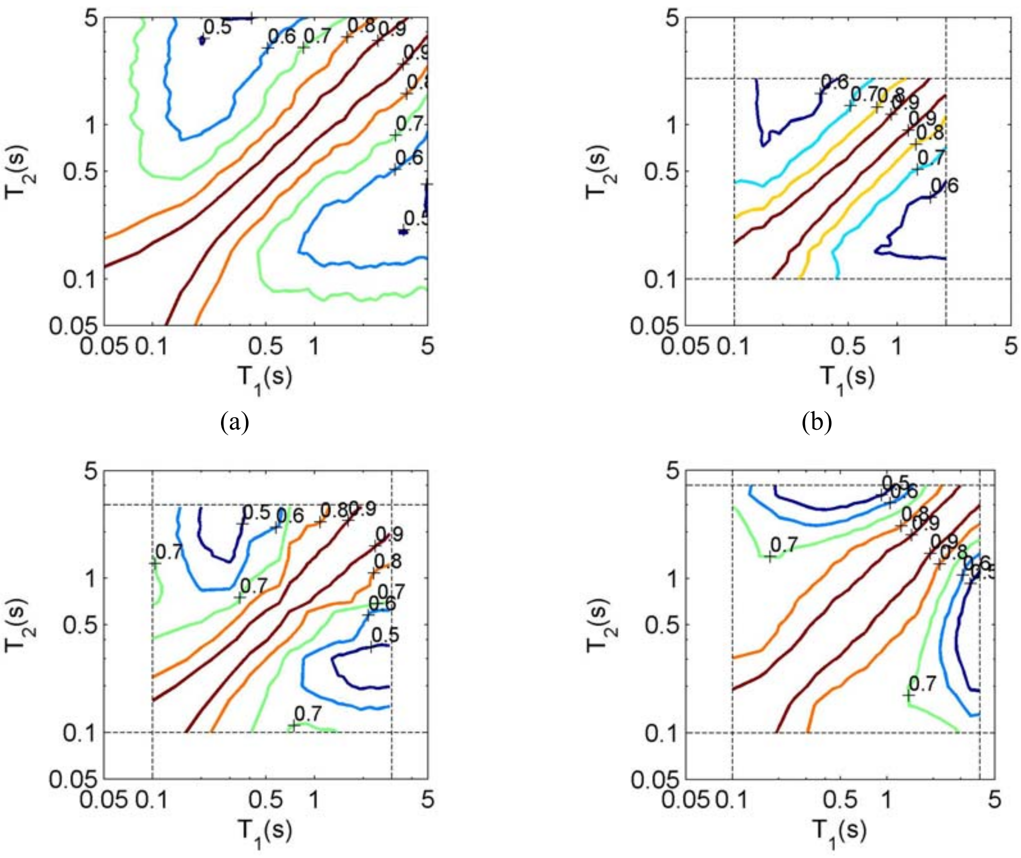

Fig. 2 Empirical correlation coefficient $\rho_{\varepsilon(T_1),\varepsilon(T_2)}$, as a function of the considered period values T_1 and T_2, calculated for V_{EIa} using the following GMPEs: (a) Cheng *et al*. (2014), (b) Chapman (1999), (c) Gong and Xie (2005), (d) Danciu and Tselentis (2007); in each plot, a range of periods that is consistent with the used GMPE is considered

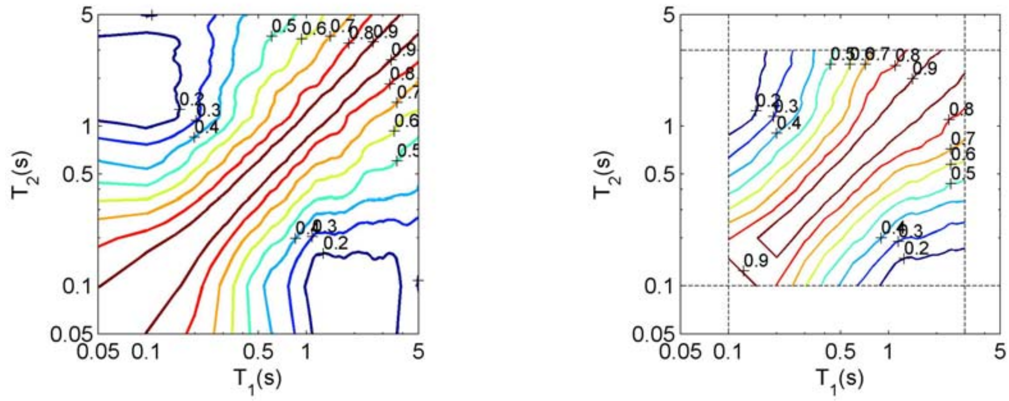

(a) (b)

Fig. 3 Empirical correlation coefficient $\rho_{\varepsilon(T_1),\varepsilon(T_2)}$, as a function of the considered period values T_1 and T_2, calculated for V_{EIr} using the following GMPEs: (a) Cheng *et al*. (2014), (b) Gong and Xie (2005)

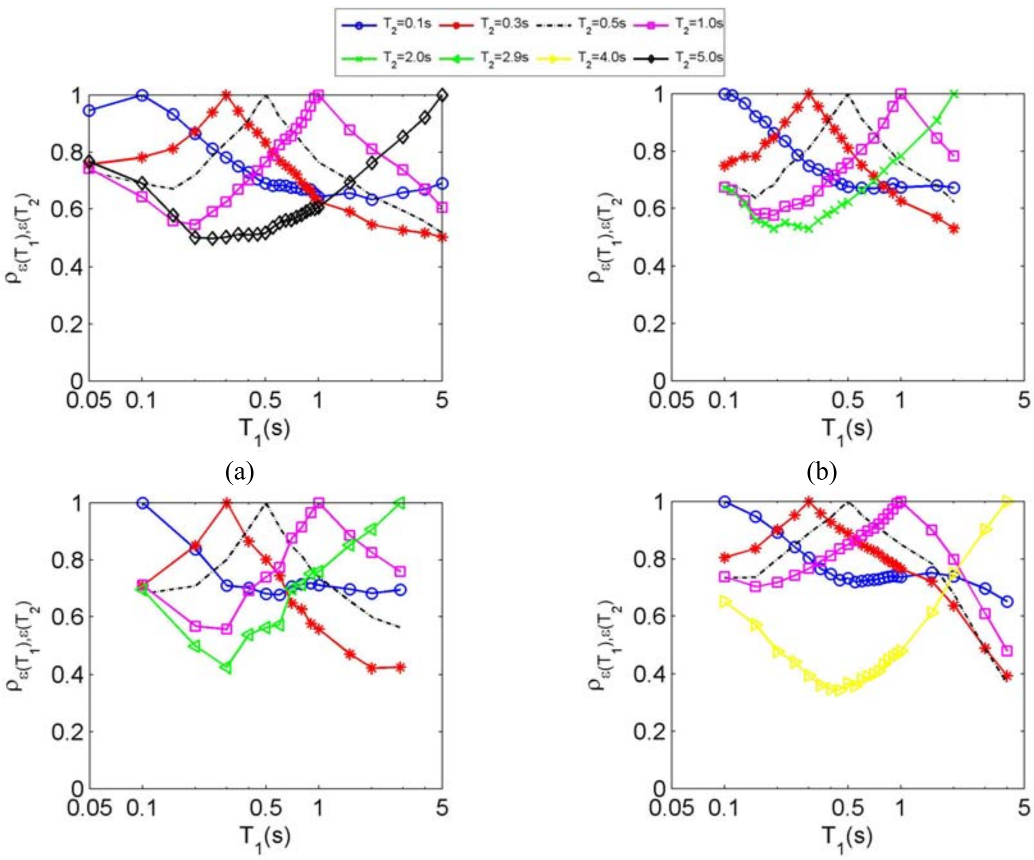

(a) (b) (c) (d)

Fig. 4 Empirical correlation coefficient $\rho_{\varepsilon(T_1),\varepsilon(T_2)}$, as a function of T_1 for different fixed values of T_2, calculated for V_{EIa} using the following GMPEs: (a) Cheng *et al*. (2014), (b) Chapman (1999), (c) Gong and Xie (2005), (d) Danciu and Tselentis (2007)

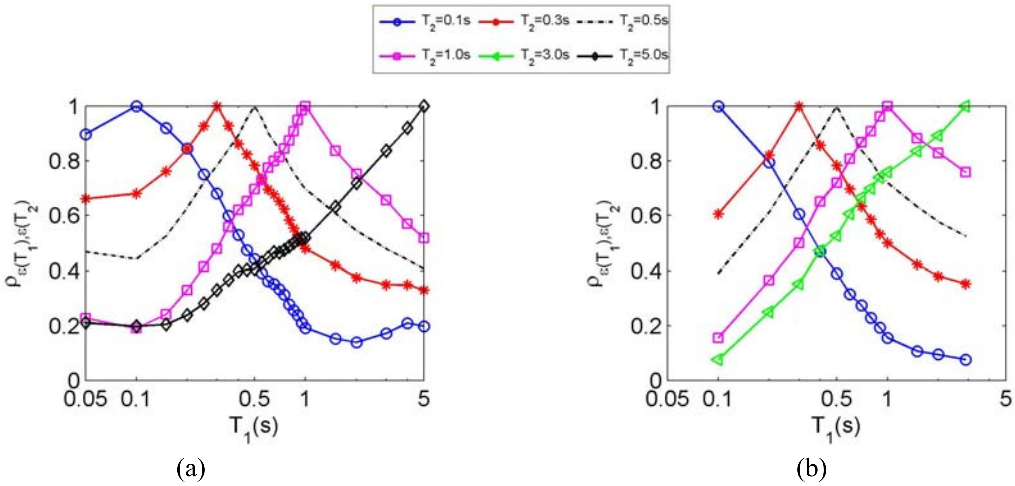

Fig. 5 Empirical correlation coefficient $\rho_{\varepsilon(T_1),\varepsilon(T_2)}$, as a function of T_1 for different fixed values of T_2, calculated for V_{EIr} using the following GMPEs: (a) Cheng *et al*. (2014), (b) Gong and Xie (2005)

Based on the empirical values obtained for the correlation coefficients, the predictive equations can be derived by fitting the given data with a selected analytical equation (see for example Baker and Cornell 2006a, Baker and Jayaram 2008, Abrahamson *et al*. 2003, Cimellaro 2013). In this work, the same nonlinear regression process as that applied in Baker and Cornell (2006a) is used. First, a Fisher's z-transformation (Neter *et al*. 1996) is applied to the correlation coefficients values (see Eq. (12)), and then the parameters of the predictive model are calibrated with a nonlinear least-squares regression, such that the squared prediction errors are minimized (see Eq. (13)). The Fisher's ztransformation is applied before the nonlinear least-squares regression for obtaining an approximate constant error for all values of the population correlation coefficients, which otherwise would be dependent on the difference between fitted and observed values (see Baker and Cornell 2006a, Baker and Jayaram 2008).

$$z_{i,j} = 0.5\ln(\frac{1+\rho_{i,j}}{1-\rho_{i,j}}) \tag{12}$$

$$\min \sum_{i=1}^{n}\sum_{j=1}^{n}(z_{i,j} - \hat{z}_{i,j})^2 \tag{13}$$

where

$\rho_{i,j}$ is the empirical correlation coefficient of ε for the T_i and T_j period values;

$z_{i,j}$ is the transformed value of the empirical correlation coefficient;

$\hat{z}_{i,j}$ is the transformed value of the the predicted correlation coefficient.

Several models for predicting the correlation between response spectra ordinates corresponding to different periods and components can be found in the literature (e.g., Abrahamson *et al*. 2003, Baker and Cornell 2006a, Baker and Jayaram 2008, Cimellaro 2013). In the present study, three different functional forms are used to develop the predictive equations: two are selected from the literature, namely, the widely used functional form of Baker and Cornell (2006a) and that based on Taylor series rationales of Cimellaro (2013); a new functional form is also proposed.

The predictive model for the correlation coefficients with the functional form proposed by Baker and Cornell (2006a) is

$$\rho_{\varepsilon(T_1),\varepsilon(T_2)} = 1 - \cos\left(\frac{\pi}{2} - (A0 + A1 \cdot I_{(T\min<A2)} \ln(\frac{T_{\min}}{A2}))\ln(\frac{T_{\max}}{T_{\min}})\right) \tag{14}$$

where: $T_{\min}$=min(T_1,T_2); $T_{\max}$=max(T_1,T_2); I is an indicator that is equal to 1 if $T_{\min}$<$A2$ and equal to 0 otherwise. In, Table 1, the values of the model parameters resulted from fitting the observed data are given. A comparison between empirical and predicted correlation coefficients for V_{EIa} and V_{EIr} is shown in Fig. 6(a) and 6(b), respectively.

The predictive model built with the functional form proposed by Cimellaro (2013) is

$$\rho_{\varepsilon(T_1),\varepsilon(T_2)} = 1 - \left(\frac{a + b\ln(T_{\min}) + c(\ln(T_{\max}))^2}{1 + d\ln(T_{\max}) + e(\ln(T_{\min}))^2}\right)\ln\left(\frac{T_{\min}}{T_{\max}}\right) \tag{15}$$

where again $T_{\min}$=min(T_1,T_2), and $T_{\max}$=max(T_1, T_2). The values of the model parameters obtained by fitting the empirical correlation coefficients are reported in Table 2. In Fig. 6(c) and 6(d) the empirical and predicted correlation coefficients for V_{EIa} and V_{EIr} are compared.

In order to improve the result of the fitting, the following new predictive model, which mixed the functional form of Baker and Cornell (2006a) with that of Cimellaro (2013), is also considered

$$\rho_{\varepsilon(T_1),\varepsilon(T_2)} = 1 - \cos\left(\frac{\pi}{2} - (B1 + A1 \cdot I_{(T\min<A2)} \ln(\frac{T_{\min}}{A2}))\ln(\frac{T_{\max}}{T_{\min}})\right) \tag{16}$$

with

$$B1 = -\frac{a + b\ln(T_{\min}) + c(\ln(T_{\max}))^2}{1 + d\ln(T_{\max}) + e(\ln(T_{\min}))^2} \tag{17}$$

and where I is equal to 1 when $T_{\min}$<$A2$ and equal to 0 otherwise. The proposed model degenerates into the model of Cimellaro (2013) when $T_{\min}$>$A2$, and into that of Baker and Cornell (2006a) when $T_{\min}$<$A2$. The calibrated parameters of the proposed model are listed in Table 3, Empirical and predicted values of the correlation coefficient are compared in Fig. 7.

Table 1 Calibration results for the predictive model of $\rho_{\varepsilon(T_1),\varepsilon(T_2)}$ built with the functional form of Baker and Cornell (2006a)

Parameters	$A0$	$A1$	$A2$
V_{EIa}	0.2665	0.1030	0.327
V_{EIr}	0.3535	0.1333	0.112

Table 2 Calibration results for the predictive model of $\rho_{\varepsilon(T_1),\varepsilon(T_2)}$ built with the functional form of Cimellaro (2013)

Parameters	a	b	c	d	e
V_{EIa}	-0.3741	-0.0628	0.0077	0.3854	0.0982
V_{EIr}	-0.4494	-0.0363	0.0393	0.1785	0.0287

Table 3 Calibration results for the predictive model of $\rho_{\varepsilon(T_1),\varepsilon(T_2)}$ built with the proposed functional form

Parameters	$A1$	$A2$	a	b	c	d	e
V_{EIa}	0.0459	0.228	-0.3464	-0.0359	0.0077	0.2796	0.0569
V_{EIr}	0.0801	0.1	-0.4368	-0.0215	0.0426	0.1109	0.0060

Table 4 AIC values for the three considered predictive models of $\rho_{\varepsilon(T_1),\varepsilon(T_2)}$

AIC	Baker and Cornell (2006a)	Cimellaro (2013)	Proposed in this study
V_{EIa}	-6314.254	-8272.737	-9087.155
V_{EIr}	-6599.84	-9053.089	-9069.951

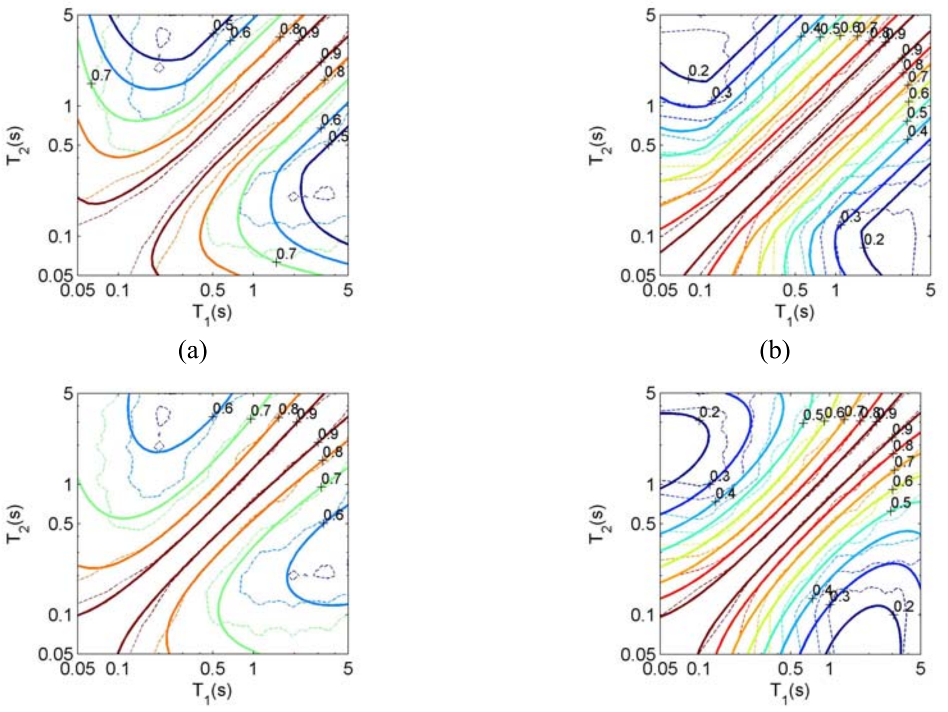

Fig. 6 Comparison between empirical (dashed lines) and predicted (solid lines) values of $\rho_{\varepsilon(T_1),\varepsilon(T_2)}$ obtained for V_{EIa} (plots on the left) and V_{EIr} (plots on the right) using the functional form of Baker and Cornell (2006a) (plots a and b) and that of Cimellaro (2013) (plots c and d)

The relative quality of these three models in predicting the correlation coefficients can be evaluated with the Akaike's Information Criterion (*AIC*, see Akaike 1974). According to this criterion, the preferred predictive model, among a set, is the one with the minimum *AIC* value, with the *AIC* being calculated as follows

$$AIC = 2k - 2\ln L \tag{18}$$

in which k is the number of model parameters, and L is the maximized likelihood value for the

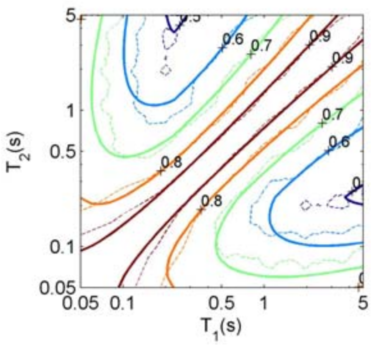

(a)

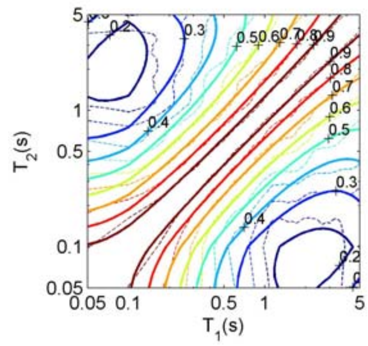

(b)

Fig. 7 Comparison between empirical (dashed lines) and predicted (solid lines) values of $\rho_{\varepsilon(T_1),\varepsilon(T_2)}$ obtained for V_{EIa} (left plot) and V_{EIr} (right plot) using the proposed functional form

model.

AIC does not only measures the goodness of fit (the "-2ln*L*" term in Eq. (18) rewards the fit between the model and the data), but also includes a penalty for including extra parameters in the model (with the "2*k*" term). It is well known that the goodness of fit can always be improved by increasing the number of model parameters. However, this improvement may be due to overfitting problems. By selecting the predicitve model that minimizes the *AIC* value, the latter are avoided and a good fit is obtained.

As shown from the results reported in Table 4, the model corresponding to the highest *AIC* value is the one which uses the functional form of Baker and Cornell (2006a), while the lowest *AIC* value is obtained with the proposed model. Based on these results and on those of Fig. 6 and Fig. 7, it can be concluded that: the best predictions are in general those obtained with the proposed equations; the empirical correlation coefficients obtained for both V_{EIa} and V_{EIr} are better fitted with the proposed model than the functional form of Baker and Cornell (2006a); for the case of V_{EIa} the prediction improves by using the proposed model instead of the functional form of Cimellaro (2013).

4.2 Correlation between spectral ordinates for orthogonal horizontal components

The same approach adopted in Baker and Cornell (2006a) is used to fit the the empirical values of $\rho_{\varepsilon_x(T),\varepsilon_y(T)}$ using a simple linear model. By looking at the plots of Fig. 8, it can be observed that the correlation coefficient obtained for V_{EIa} does not significantly vary with period. The slope of the linear model, in fact, is very small. Because of that, the correlation can be approximately calculated as follows

$$\rho_{\varepsilon_x(T),\varepsilon_y(T)} = 0.864 \tag{19}$$

where *x* and *y* indicate the two orthogonal horizontal ground motion componennts.

For the case of V_{EIr}, instead, the dependency of the correlation coefficient on period is not negligible, and the following equation can be used for the prediction

$$\rho_{\varepsilon_x(T),\varepsilon_y(T)} = 0.839 - 0.0288\ln(T) \tag{20}$$

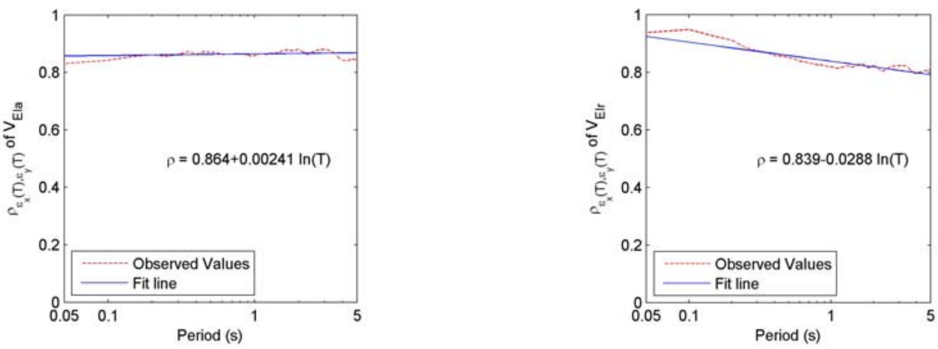

(a) (b)

Fig. 8 Comparison between empirical (dashed red lines) and predicted (solid blue lines) values of $\rho_{\varepsilon_x(T),\varepsilon_y(T)}$ obtained for V_{EIa} (left plot) and V_{EIr} (right plot) using a linear model

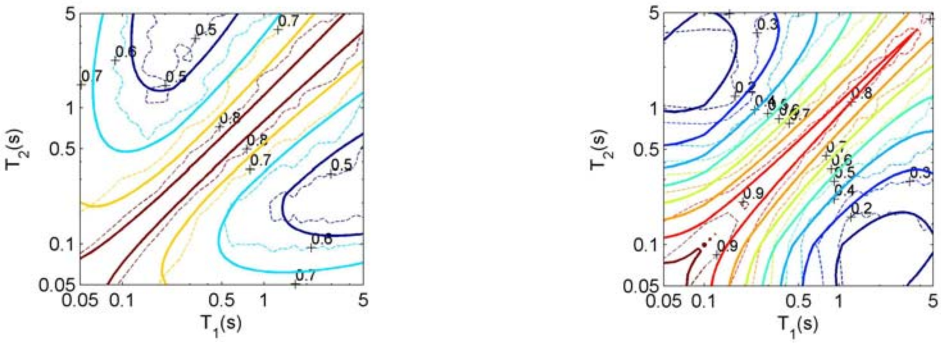

(a) (b)

Fig. 9 Comparison between empirical (dashed lines) and predicted (solid lines) values of $\rho_{\varepsilon_x(T_1),\varepsilon_y(T_2)}$ obtained for V_{EIa} (left plot) and V_{EIr} (right plot) using Eq. (21) and Eq. (22), respectively

Analogously to what is done in Baker and Cornell (2006a) and Baker and Jayaram (2008), the correlation coefficient $\rho_{\varepsilon_x(T_1),\varepsilon_y(T_2)}$ for spectral values corresponding to different periods and components is estimated by multiplying $\rho_{\varepsilon_x(T),\varepsilon_y(T)}$ (correlation coefficient for different components and same period value) with $\rho_{\varepsilon(T_1),\varepsilon(T_2)}$ (correlation coefficient for different periods and the same component). Therefore, for V_{EIa} and V_{EIr} $\rho_{\varepsilon_x(T_1),\varepsilon_y(T_2)}$ is respectively given by the two following equations

$$\rho_{\varepsilon_x(T_1),\varepsilon_y(T_2)} = 0.864\rho_{\varepsilon(T_1),\varepsilon(T_2)} \tag{21}$$

$$\rho_{\varepsilon_x(T_1),\varepsilon_y(T_2)} = (0.839 - 0.0288\ln\sqrt{T_1T_2})\rho_{\varepsilon(T_1),\varepsilon(T_2)} \tag{22}$$

where $\rho_{\varepsilon_x(T_1),\varepsilon_y(T_2)}$ is calculated with Eq. (16). Note that ln(T) of Eq. (20) is replaced in Eq. (22) by the arithmetic mean of the logarith of the two periods of interest.

In Fig. 9, a comparison between empirical and predicted values of $\rho_{\varepsilon_x(T_1),\varepsilon_y(T_2)}$ is reported for both V_{EIa} and V_{EIr}. It can be observed that the predictive equations fit well the observed data.

5. Applications of the proposed predictive equations

In this section of the paper, some possible applications of the proposed predictive equations are discussed. In particular, the use of the equations for predicting V_{EI}-derived IMs and for calculating conditional mean spectra is shown.

5.1 Prediction of V_{EI}-derived IM

The predictive equations for the correlation coefficients investigated in this study can be used to predict V_{EI}-derived IMs such as $V_{EIa}SI$, $V_{EIr}SI$, $MV_{EIa}SI$ and $MV_{EIr}SI$ (see Table 5 for definitions), which have been shown to be good predictors for some types of structures and response parameters of interest (e.g., see Mollaioli et al. 2013). $V_{EIa}SI$ and $V_{EIr}SI$ are obtained by integrating from 0.1s to 3.0s V_{EIa} and V_{EIr}, respectively. $MV_{EIa}SI$ and $MV_{EIr}SI$ are modified versions of $V_{EIa}SI$ and $V_{EIr}SI$, with the period range of integration determined based on the dynamic properties of the structure. By changing the period range of integration, in fact, the predictive performance of these IMs can be improved. In order to predict these V_{EI}-derived by means of GMPEs, regression analyses as those reported in Cheng *et al*. (2014) could be carried out. This means that for the case of the structure-specific IMs $MV_{EIa}SI$ and $MV_{EIr}SI$, regression analyses as many as the number of integration ranges of interests should be carried out. As an alternative, instead of a direct prediction the method proposed in Bradley *et al*. (2009) can be used. According to this method, which was developed for predicting the Housner intensity (Housner 1952) based on GMPE for the pseudo-velocity *Spv*, median and standard deviation of the generic integral energy-based IM $V_{EI}SI$ can be calculated as follows

$$\mu_{V_{EI}SI} = \Delta T \sum_{i=1}^{n} w_i \mu_{V_{EI}i} \tag{23}$$

$$\sigma_{V_{EI}SI} = (\Delta T)^2 \sum_{i=1}^{n} \sum_{j=1}^{n} (w_i w_j \rho_{V_{EI}i,V_{EI}j} \sigma_{V_{EI}i} \sigma_{V_{EI}j}) \tag{24}$$

in which
n is the number of period values where V_{EI} is computed at;
ΔT is the size of the vibration period discretization (the step-size used in the integration));
w_i and w_j are integration weights that depend on the used integration scheme.

Based on Eq. (24), it is clear that in order to calculate the standard deviation of $V_{EI}SI$, the

Table 5 Integral energy-based IMs derived from V_{EI}

Name	Definition
Absolute elastic input energy equivalent velocity spectrum intensity	$V_{EIa}SI = \int_{0.1}^{3.0} V_{EIa}(T)dT$
Relative elastic input energy equivalent velocity spectrum intensity	$V_{EIr}SI = \int_{0.1}^{3.0} V_{EIr}(T)dT$
Modified $V_{EIa}SI$	$MV_{EIa}SI = \int_{0.2T}^{1.5T} V_{EIa}(T)dT$
Modified $V_{EIr}SI$	$MV_{EIr}SI = \int_{0.2T}^{1.5T} V_{EIr}(T)dT$

correlation coefficients $\rho_{V_{EI}i,V_{EI}j}$ of V_{EI} at different periods is needed. Thus, by using Eq. (23), Eq. (24) and the proposed equations, together with prediction equations for V_{EI}, $V_{EIa}SI$, $V_{EIr}SI$, $MV_{EIa}SI$ and $MV_{EIr}SI$ (as well as similar integral energy-based IMs derived from V_{EI}) can be simply predicted without the need of developing any other additional GMPE.

5.2 Development of conditional mean spectrum

A uniform hazard spectrum (UHS) is a response spectrum with ordinates characterized by the same probability of being exceeded. It is computed using probabilistic seismic hazard analysis, and in the case of assessment procedures requiring dynamic analyses for the seismic demand evaluation of structures used as a target for the selection of earthquake ground motions. A UHS does not look like observed spectra, and does not represent the expected spectrum for the causal earthquake event. Recently, studies showed that UHS is not appropriate for probabilistic seismic demand analysis, due to the fact that it conservatively assumes that a single ground motion may have extremely large amplitudes at all frequencies (e.g., see Baker and Cornell 2006a). Because of that, alternative target spectra have been proposed. Among them, a target spectrum which has been shown to be superior for obtaining unbiased estimates of structural response is the conditional mean spectrum (CMS) (Baker 2011). The CMS is defined as the expected response spectrum conditioned on occurrence of a target spectral value at the period of interest. In order to calculate it, the correlation of spectral values at different periods is needed (see Baker 2011). Thus, the predictive equations proposed in this study can be used for calculating the CMS of V_{EIa} and V_{EIr}. In particular, for the considered equivalent velocity V_{EI}, the conditional mean value of $\ln V_{EI}$ at period T_i conditioned on the value of $\ln V_{EI}$ at period T^* can be computed using the following equation

$$\mu_{\ln V_{EI}(T_i)|\ln V_{EI}(T^*)} = \mu_{\ln V_{EI}(T_i)}\left(\overline{M},\overline{R},T_i,\overline{\theta}\right) + \rho_{\varepsilon(T_i),\varepsilon(T^*)} \cdot \varepsilon\left(T^*\right) \cdot \sigma_{\ln V_{EI}}\left(T_i\right) \tag{25}$$

where

$\mu_{\ln V_{EI}(T_i)}\left(\overline{M},\overline{R},T_i,\overline{\theta}\right)$ and $\sigma_{\ln V_{EI}}\left(T_i\right)$ are the predicted median and standard deviation of $\ln V_{EI}(T_i)$ obtained with the GMPE (e.g., the one proposed in Cheng *et al*. 2014);

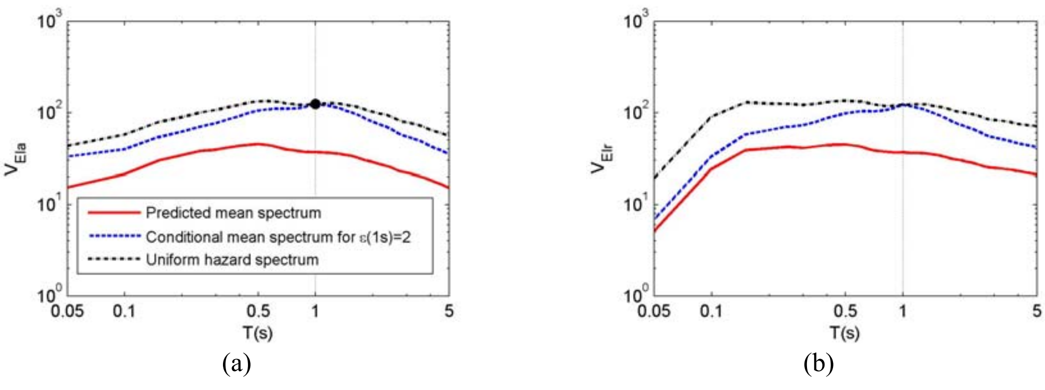

Fig. 10 CMS of V_{EIa} (a) and V_{EIr} (b) conditioned on ε(1s)=2, compared with predicted median spectra obtained with the GMPE of Cheng *et al*. (2014) and with UHS

$\bar{\theta}$ denotes model parameters other than magnitude M and distance R, such as parameters related to soil condition and fault mechanism;

$\rho_{\varepsilon(T_i),\varepsilon(T^*)}$ is the correlation coefficient of epsilon at different periods for the same component, which can be calculated using Eq. (16) and Eq. (17).

Fig. 10 shows CMS of V_{EIa} and V_{EIr}, obtained with the GMPE proposed in Cheng *et al*. (2014), along with their UHS and median spectra. In this example, the period of interest T^* is equal to 1s, and the target spectral value is equal to the predicted median plus two standard deviations. It is interesting to observe that V_{EIa} and V_{EIr} are close to each other around T equal to 1s; at lower periods, instead, V_{EIr} is lower than V_{EIa} due to the relative lower correlation of the V_{EIr} spectral values in this range of periods.

6. Conclusions

In this study, models for predicting the correlation between spectral values of two energy-based earthquake intensity measures, namely, the absolute and the relative elastic input energy equivalent velocity (V_{EIa} and V_{EIr}, respectively), were developed. For both V_{EIa} and V_{EIr}, three different correlations coefficients were investigated: the correlation coefficient between two ordinates of the equivalent velocity spectrum of the single horizontal component of the ground motion; the correlation coefficient between the ordinates of the spectra of the two orthogonal horizontal components calculated at the same period value; the correlation coefficient between the ordinates of the spectra of the two orthogonal horizontal components calculated at two different periods.

Different functional forms for the predictive models were investigated. Among them, a proposed functional form and a functional form used in Cimellaro (2013) were found to better fit empirical correlation coefficients obtained from a dataset of ground motion records. In particular, for the case of V_{EIr} a good fit was obtained for both functional forms, while for the case of V_{EIa} improved prediction were obtained by using the proposed one.

The proposed predictive equations can be applied in seismic hazard analysis problems and in ground motion selection and modification methods. For example, as shown in the previous section of the paper, they can be used to predict energy-based intensity measures derived from V_{EIa} and V_{EIr}, such as $V_{EIa}SI$, $V_{EIr}SI$, $MV_{EIa}SI$ and $MV_{EIr}SI$, and also to calculate the conditional mean spectrum of V_{EIa} and V_{EIr}. The latter can be then used as target spectrum for ground motion selection and modification methods and used in assessment or design analysis where the evaluation of both the displacement and the energy demand in the structure is of interest.

It is important to note that these models are strictly empirical, and thus their use should not be extrapolated beyond the range over which the observed values were fit. This means that the proposed predictive models should be used only for period values ranging between 0.05 s and 5 s, earthquake magnitude range of 5-7.9, fault-to-site closest distance less than 200 km, and NEHRP soil conditions class B, C and D.

Acknowledgments

The financial support of both the Italian Ministry of the Instruction, University and Research (MIUR) and the Italian Network of University Laboratories of Seismic Engineering (ReLUIS) is gratefully acknowledged.

References

Abrahamson, N.A., Kammerer, A. and Gregor, N. (2003), "Summary of scaling relations for spectral damping, peak velocity, and average spectral acceleration", Report for the PEGA-SOS project, Personal communication.

Akaike, H. (1974), "A new look at the statistical model identification", *IEEE Trans. Automatic Control*, **19**(6), 716-723.

Akiyama, H. (1985), *Earthquake resistant limit-state design for buildings*, Univ. Tokyo Press, Tokyo.

Baker, J. (2011), "Conditional mean spectrum: tool for ground-motion selection", *J. Struct. Eng.*, **137**(3), 322-331.

Baker, J. and Cornell, C.A. (2006a), "Correlation of response spectral values for multicomponent ground motions", *Bull. Seismol. Soc. Am.*, **96**(1), 215-227.

Baker, J. and Cornell, C.A. (2006b), "Spectral shape, epsilon and record selection", *Earthq. Eng. Struct. Dyn.*, **35**(9), 1077-1095.

Baker, J. and Jayaram, N. (2008), "Correlation of spectral acceleration values from NGA ground motion models", *Earthq. Spectra*, **24**(1), 299-317.

Benavent-Climent, A., López-Almansa, F. and Bravo-González, D.A. (2010), "Design energy input spectra for moderate-to-high seismicity regions based on Colombian earthquakes", *Soil Dyn. Earthq. Eng.*, **30**(11), 1129-1148.

Bertero, V.V. and Uang, C.M. (1992), *Issues and future directions in the use of energy approach for seismic-resistant design of structures*, *Nonlinear seismic analysis of reinforced concrete buildings*, Elsevier, London.

Bradley, A.B., Cubrinovski, M., MacRae, G.A. and Dhakal, R.P. (2009), "Ground-motion prediction equation for SI based on spectral acceleration equations", *Bull. Seismol. Soc. Am*., **99**(1), 277-285.

Chai, R.Y.H. and Fajfar, P.A. (2000), "Procedure for estimating input energy spectra for seismic design", *J. Earthq. Eng.*, **4**(4), 539-561.

Chapman, M.C. (1999), "On the use of elastic input energy for seismic hazard analysis", *Earthq. Spectra*, **15**(4), 607-635.

Cheng, Y., Lucchini, A. and Mollaioli, F. (2014), "Proposal of new ground-motion prediction equations for elastic input energy spectra", *Earthq. Struct*., **7**(4), 485-510.

Chou, C.C. and Uang, C.M. (2000), "Establishing absorbed energy spectra-an attenuation approach", *Earthq. Eng. Struct. Dyn.*, **29**(10), 1441-1455.

Chou, C.C. and Uang, C.M. (2003), "A procedure for evaluation of seismic energy demand of framed structures", *Earthq. Eng. Struct. Dyn.*, **32**(2), 229-244.

Cimellaro, G.P. (2013), "Correlation in spectral acceleration for earthquakes in Europe", *Earthq. Eng. Struct. Dyn.*, **42**(4), 623-633.

Danciu, L. and Tselentis, G.A. (2007), "Engineering ground-motion parameters attenuation relationships for Greece", *Bull. Seismol. Soc. Am*., **97**(1), 162.

Decanini, L.D. and Mollaioli, F. (1998), "Toward the definition of the relation between hysteretic and input energy", *Proceeding of 6th U.S. National Conference on Earthquake Engineering*, EERI, Oakland, California.

Decanini, L.D. and Mollaioli, F. (2001), "An energy-based methodology for the assessment of seismic demand", *Soil Dyn. Earthq. Eng.*, **21**(2), 113-137.

Fajfar, P. and Fischinger, M. (1990), "A seismic procedure including energy concept", *Proceedings of IX ECEE*, Moscow, September.

Fajfar, P. and Vidic, T. (1994), "Consistent inelastic design spectra: hysteretic and input energy", *Earthq. Eng. Struct. Dyn.*, **23**(5), 523-537.

Gong, M.S. and Xie, L.L. (2005), "Study on comparison between absolute and relative input energy spectra and effects of ductility factor", *Acta. Seismol. Sinic.*, **18**(6), 717-726.

Haselton, C.B., Baker, J.W., Bozorgnia, Y., Goulet, C.A., Kalkan, E., Luco, N., Shantz, T., Shome, N., Stewart, J.P., Tothong, P., Watson-Lamprey, J. and Zareian, F. (2009), "Evaluation of ground motion selection and modification methods: Predicting median interstory drift response of buildings", PEER Report 2009/01 College of Engineering University of California, Berkeley.

Housner, G.W. (1952), "Spectrum intensities of strong motion earthquakes", *Proceedings of Symposium of earthquake and blast effects on structures*, EERI, Los Angeles, California.

Jayaram, N., Mollaioli, F., Bazzurro, P., De Sortis, A. and Bruno, S. (2010), "Prediction of structural response of reinforced concrete frames subjected to earthquake ground motions", *9th U.S. National and 10th Canadian Conference on Earthquake Engineering*, Toronto, Canada.

Krawinkler, H. (1987), "Performance assessment of steel components", *Earthq. Spectra*, **3**(1), 27-41.

López-Almansa, F., Yazgan, A. and Benavent-Climent, A. (2013), "Design energy input spectra for high seismicity regions based on turkish registers", *Bull. Earthq. Eng.*, **11**(4), 885-912.

Lucchini, A., Mollaioli, F. and Monti, G. (2011), "Intensity measures for response prediction of a torsional building subjected to bi-directional earthquake ground motion", *Bull. Earthq. Eng.*, **9**(5), 1499-1518.

Luco, N., Manuel, L, Baldava, S. and Bazzurro, P. (2005), "Correlation of damage of steel moment-resisting frames to a vector-valued ground motion parameter set that includes energy demands", *Proceedings of the 9th International Conference on Structural Safety and Reliability*, ICOSSAR05.

Manfredi, G. (2001), "Evaluation of seismic energy demand", *Earthq. Eng. Struct. Dyn.*, **30**(4), 485-499.

Decanini, L.D. and Mollaioli, F. (2001), "An energy-based methodology for the assessment of seismic demand", *Soil Dyn. Earthq. Eng.*, **21**(2), 113-137.

McCabe, S.L. and Hall, W.J. (1989), "Assessment of seismic structural damage", *J. Struct. Eng.*, **115**(9), 2166-2183.

Mollaioli, F., Bruno, S., Decanini, L. and Saragoni, R. (2011), "Correlation between energy and displacment demand for performance-based seismic engineering", *Pure Appl. Geophys.*, **168**(2011), 237-259.

Yakut, A. and Yilmaz, H. (2008), "Correlation of deformation demands with ground motion intensity", *J. Struct. Eng.*, **134**(12), 1818-1828.

Mollaioli, F., Lucchini, A., Cheng, Y. and Monti, G. (2013), "Intensity measures for the seismic response prediction of base-isolated buildings", *Bull. Earthq. Eng.*, **11**(5), 1841-1866.

Neter, J., Kutner, M.H., Nachtsheim, C.J. and Wasserman, W. (1996), *Applied linear statistical models*, MacGraw-Hill, Boston, Massachusetts, USA.

Teran-Gilmore, A. (1996), "Performance-based earthquake-resistant design of framed buildings using energy concepts", Ph.D. Dissertation, Department of Civil Engineering, University of California at Berkeley.

Uang, C.M. and Bertero, V.V. (1990), "Evaluation of seismic energy in structures", *Earthq. Eng. Struct. Dyn.*, **19**(1), 77-90.

IT

Appendix

Table A Symbols and acronyms used in this article

IM	Intensity measure
GMPE	Ground motion prediction equation
Sa	pseudo-acceleration
Spv	pseudo-velocity
PGA	Peak ground acceleration
PGV	Peak ground velocity
$MIDR$	Maximum inter-story drift ratio
V_{EIa}	Absolute elastic input energy equivalent velocity
V_{EIr}	Relative elastic input energy equivalent velocity
V_{EI}	Relative or absolute elastic input energy equivalent velocity
SDOF	Single-degree-of-freedom
E_{Ia}	Absolute elastic input energy
E_{Ir}	Relative elastic input energy
E_a	Absorbed energy
NEHRP	National earthquake hazards reduction program
NGA	Next generation attenuation
AIC	Akaike's information criterion
CMS	Conditional mean spectrum
EDP	Engineering demand parameter
$V_{EIa}SI$	Absolute elastic input energy equivalent velocity spectrum intensity
$V_{EIr}SI$	Relative elastic input energy equivalent velocity spectrum intensity
$MV_{EIa}SI$	Modified $V_{EIa}SI$
$MV_{EIr}SI$	Modified $V_{EIr}SI$
UHS	Uniform hazard spectrum

Table B Info about the earthquakes considered in this study

Earthquake name	Year	Mag.	Hyp. depth (km)	Mechanism	No. of records	Site B	Site C	Site D
San Fernando	1971	6.61	13	Reverse	7	1	3	3
Friuli, Italy-01	1976	6.50	5.1	Reverse	4	0	3	1
Gazli, USSR	1976	6.80	18.2	Reverse	1	0	1	0
Coyote Lake	1979	5.74	9.6	Strike - Slip	4	0	1	3
Imperial Valley-06	1979	6.53	9.96	Strike - Slip	24	0	1	23
Livermore-01	1980	5.80	12	Strike - Slip	1	0	1	0
Mammoth Lakes-01	1980	6.06	9	Normal	1	0	0	1
Victoria, Mexico	1980	6.33	11	Strike - Slip	4	0	1	3
Irpinia, Italy-01	1980	6.90	9.5	Normal	6	3	3	0
Westmorland	1981	5.90	2.3	Strike - Slip	3	0	0	3

Table B Continued

Earthquake name	Year	Mag.	Hyp. depth (km)	Mechanism	No. of records	Site B	Site C	Site D
Coalinga-01	1983	6.36	4.6	Reverse	37	0	22	15
Morgan Hill	1984	6.19	8.5	Strike - Slip	17	1	5	11
Nahanni, Canada	1985	6.76	8	Reverse	2	0	2	0
Hollister-04	1986	5.45	8.72	Strike - Slip	1	0	0	1
N. Palm Springs	1986	6.06	11	Reverse	7	0	1	6
Chalfant Valley-01	1986	5.77	6.7	Strike - Slip	9	0	0	9
Whittier Narrows-01	1987	5.99	14.6	Reverse	2	0	0	2
Superstition Hills-01	1987	6.22	10	Strike - Slip	1	0	0	1
Superstition Hills-02	1987	6.54	9	Strike - Slip	3	0	0	3
Loma Prieta	1989	6.93	17.48	Reverse	51	6	24	21
Cape Mendocino	1992	7.01	9.6	Reverse	5	0	3	2
Landers	1992	7.28	7	Strike - Slip	41	0	8	33
Big Bear-01	1992	6.46	13	Strike - Slip	11	0	4	7
Northridge-01	1994	6.69	17.5	Reverse	91	7	44	40
Kobe, Japan	1995	6.90	17.9	Strike - Slip	2	0	1	1
Dinar, Turkey	1995	6.40	5	Normal	1	0	0	1
Kocaeli, Turkey	1999	7.51	15	Strike - Slip	7	1	1	5
Chi-Chi, Taiwan	1999	7.62	6.76	Reverse	281	2	143	136
Duzce, Turkey	1999	7.14	10	Strike - Slip	3	0	2	1
St Elias, Alaska	1979	7.54	15.7	Reverse	2	0	0	2
Sierra Madre	1991	5.61	12	Reverse	1	0	1	0
Little Skull Mtn, NV	1992	5.65	12	Normal	8	0	3	5
Hector Mine	1999	7.13	5	Strike - Slip	48	0	19	29
Yountville	2000	5.00	10.12	Strike - Slip	18	0	4	14
Mohawk Val, Portola	2001	5.17	3.95	Strike - Slip	3	0	0	3
Gulf of California	2001	5.70	10	Strike - Slip	10	0	0	10
CA/Baja Border Area	2002	5.31	7	Strike - Slip	9	0	0	9
Nenana Mountain, Alaska	2002	6.70	4.2	Strike - Slip	5	0	4	1
Denali, Alaska	2002	7.90	4.86	Strike - Slip	9	2	4	3